American Mineralogist, Volume 89, pages 232–238, 2004

Shirozulite, $KMn^{2+}_3(Si_3Al)O_{10}(OH)_2$, a new manganese-dominant trioctahedral mica: Description and crystal structure

KIYOTAKA ISHIDA,[1]* FRANK C. HAWTHORNE,[2] AND FUMITOSHI HIROWATARI[3]

[1]Department of Evolution of the Earth and the Environment, Graduate School of Social and Cultural Studies, Kyushu University, 4-2-1 Ropponmatsu, Chuo-ku, Fukuoka 810-8560, Japan
[2]Department of Geological Sciences, University of Manitoba, Winnipeg, Manitoba R3T 2N2, Canada
[3] 2734-1-1 Fukuma, Fukuoka 811-3213, Japan

ABSTRACT

Shirozulite is a new Mn-dominant trioctahedral mica from the Taguchi mine, Aichi Prefecture, Japan. The mineral occurs in tephroite-rhodochrosite ores in contact with a Ba-bearing, K-feldspar vein. Shirozulite formed during regional low-*P*/*T* metamorphism and, thereafter, suffered thermal metamorphism from a local granodiorite. Grains of shirozulite are up to 0.5 mm across and have a typical micaceous habit. Color: dark reddish brown. Cleavage: (001), perfect. Optical properties: biaxial negative, $2V_x$ = very small. Strongly pleochroic: X = pale yellow, Y = Z = pale brown, absorption X < Y ≈ Z. Refractive indices: $n_\alpha = 1.592(2)$, $n_\beta \approx n_\gamma = 1.635(2)$. The structural formula is $(K_{0.90}Ba_{0.09})(Mn^{2+}_{1.53}Mg_{0.94}Fe^{2+}_{0.20}Ti_{0.04}Al_{0.29})(Si_{2.54}\ Al_{1.46})\ O_{10}\ [(OH)_{1.97}F_{0.03}]$, and the end-member composition is $KMn^{2+}_3AlSi_3O_{10}(OH)_2$. Density: obs. = 3.20(3) g/cm^3 by pycnometer, calc. = 3.14(2) g/cm^3. Shirozulite is monoclinic, *C*2/*m*, 1M polytype, $a = 5.3791(7)$, $b = 9.319(1)$, $c = 10.2918(9)$ Å, $\beta = 100.186(9)°$, $V = 507.8(1)$ Å^3. The six strongest lines in the powder X-ray diffraction pattern are as follows: *d* (Å), *I* (%), (*hkl*): 10.16, 100, (001); 2.654, 96, ($\bar{1}$31); 3.386, 51, (003); 1.556, 48, ($\bar{3}$13); 2.467, 46, ($\bar{1}$32); 2.202, 36, ($\bar{1}$33). The crystal structure has been refined to an *R* value of 4.1% based on 663 observed reflections collected with Mo*K*α X-radiation from a single crystal. The mean bond lengths, tetrahedral rotation, and octahedral flattening angles are as follows: <T-O> = 1.668, <M1-O> = 2.118, <M2-O> = 2.103, <K-O>(inner) = 2.995, and <K-O>(outer) = 3.376 Å, $\alpha = 8.36°$, $\psi_{M1} = 58.5°$, $\psi_{M2} = 58.2°$. The apparent element distribution coefficient analyses among coexisting manganese or manganoan silicate minerals indicate that the trioctahedral mica structure cannot contain larger amounts of Mn^{2+} relative to Mg and Fe^{2+} than in olivine, pyroxenoid, and garnet.

INTRODUCTION

Trioctahedral micas along the phlogopite-annite join occur as rock-forming minerals in a wide range of geological environments. They usually contain only minor Mn^{2+}, and micas containing dominant octahedral Mn^{2+} have not been reported until now. Synthesis work on trioctahedral micas with Mn-bearing starting materials suggests that micas with a tetrahedral composition of (Si_3Al) cannot contain more than about one $^{VI}Mn^{2+}$ pfu (per formula unit) (Hazen and Wones 1972). However, a new Mn^{2+}-dominant trioctahedral mica has been found at the Taguchi mine, a regionally and thermally metamorphosed strata-bound Mn ore deposit in Aichi Prefecture, Japan. This mineral is named shirozulite in honor of Dr. Haruo Shirozu, Professor Emeritus of Kyushu University, for his outstanding contributions to the crystal-chemistry of sheet-silicate minerals, particularly the chlorite group. Shirozulite has been approved as a new mineral by the International Mineralogical Association's Committee on New Minerals and Mineral Names. Type material is deposited at the Graduate School of Social and Cultural Studies, Kyushu University, Japan.

* E-mail: kiyota@rc.kyushu-u.ac.jp

SAMPLE DESCRIPTION

Occurrence

The Taguchi mine is located at Yatuhashi, Kita-shitara County, Aichi Prefecture, Japan. The mine is in a strata-bound Mn ore deposit in the Ryoke metamorphic belt and is renowned for an abundance of mineral species: e.g., yoshimuraite (Hirowatari and Isono 1963), richterite (Shoda and Bunno 1973), alleghanyite, sonolite, manganosite, jacobsite, and galaxite. Manganese-rich layers are up to 2 m wide and show a zonal arrangement: hausmannite + rhodochrosite, tephroite, and pyroxenoid (rhodonite, pyroxmangite) ores (Hirowatari and Isono 1963). Shirozulite formed during low *P*/*T*-type regional metamorphism of Cretaceous age, and thereafter, was thermally metamorphosed by an adjacent granodiorite. Shirozulite occurs in tephroite-rhodochrosite ores in contact with a Ba-bearing K-feldspar vein, as subhedral grains closely associated with tephroite, rhodochrosite, and apatite. Grains of barite (a few μm across) and bementite (about 5 μm in diameter) are dispersed throughout the rhodochrosite, giving it a turbid appearance in thin section. A back-scattered electron image is shown in Figure 1; the mottled appearance of the mica is due to minor chemical heterogeneity involving the substitution $^{XII}Ba^{IV}Al^{XII}K_{-1}{}^{IV}Si_{-1}$.

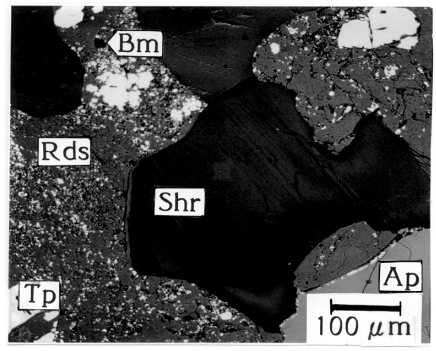

FIGURE 1. Back-scattered-electron image of shirozulite. Shr = shirozulite; Tp = tephroite; Ap = apatite; Rds = rhodochrosite; Bm = bementite.

Physical properties

Grains of shirozulite are up to 0.5 mm across and have a typical micaceous appearance. Color: dark reddish brown. Cleavage: (001) perfect. Optical properties: biaxial negative, $2V_x$ = very small. Strongly pleochroic: X = pale yellow, Y = Z = pale brown, absorption X < Y ≈ Z. Refractive indices: $n_\alpha = 1.592(2)$, $n_\beta \approx n_\gamma = 1.635(2)$. Density: obs. = 3.20 g/cm^3 by pycnometer, calc. = 3.14 g/cm^3. Vickers hardness was measured on the (001) surface with an Akashi model MVK: VHN = 100~130; Mohs hardness ≈ 3.

Chemical composition

Preliminary chemical analyses of the mica and coexisting minerals were done using a scanning electron microscope JEOL SEM35CF-II equipped with a Link System 800-2-500 energy-dispersive spectrometer and a ZAF-4/FLS quantitative-analysis software system. Operating conditions were as follows: accelerating voltage 15 kV, beam current 1.5 nA on Fe metal, and 100 s collecting time.

The crystal used to collect single-crystal XRD data was mounted in epoxy, polished, and analyzed using a CAMECA SX-50 electron-microprobe operating in wavelength-dispersion mode, with a beam diameter of 5 μm and an accelerating voltage of 15 kV. The following standards were used: albite (Na*K*α), fayalite (Fe*K*α), diopside (Ca*K*α, Si*K*α), kyanite (Al*K*α), spessartine (Mn*K*α), orthoclase (K*K*α), zinnwaldite (F*K*α), forsterite (Mg*K*α), titanite (Ti*K*α), and barite (Ba*L*α). The mean composition is given in Table 1. The value for H_2O was calculated assuming OH + F = 2 apfu (atom per formula unit). The structural formula for shirozulite is $(K_{0.90}Ba_{0.09})(Mn^{2+}_{1.53}Mg_{0.94}Fe^{2+}_{0.20}Ti_{0.04}Al_{0.29})(Si_{2.54}Al_{1.46})O_{10}[(OH)_{1.97}F_{0.03}]$, and its end-member composition is $KMn^{2+}_3(AlSi_3)O_{10}(OH)_2$.

Single-crystal diffraction and structure refinement

A crystal was mounted on a Siemens *P*4 automated four-circle diffractometer with a graphite monochromator and a Mo X-ray tube. Twenty-five reflections were centered; a constrained monoclinic cell was determined from the setting angles and refined using a least-squares technique (Table 2). Single-crystal intensity data were measured from 4 to 60 °2θ with a scan range of 1.2° and scan-speeds from 2.5 to 29.3 °/min. Psi-scan data were measured on 20 reflections out to 60 °2θ at increments of 5°; an absorption correction was done with the crystal modeled as a thin plate.

TABLE 1. Chemical analysis (in wt%) and formula unit* for shirozulite

SiO_2	31.40	Si	2.536
Al_2O_3	18.45	Al	1.464
TiO_2	0.71	Σ	4.000
FeO	2.90		
MnO	22.38	Ti	0.043
MgO	7.83	Al	0.292
BaO	2.77	Fe^{2+}	0.196
K_2O	8.75	Mg	0.943
F	0.11	Mn^{2+}	1.531
H_2O†	3.66	Σ	3.005
O = F	–0.05		
Σ	98.91	K	0.902
		Ba	0.088
		Σ	0.990
		OH	1.972
		F	0.028
		Σ	2.000

* Calculated on the basis of 12 anions with (OH + F) = 2.00 apfu.
† Determined by stoichiometry.

TABLE 2. Unit-cell dimensions and data pertaining to crystal-structure refinement of shirozulite

a (Å)	5.3791(7)	crystal size (mm)	0.06 × 0.10 × 0.16
b (Å)	9.319(1)	radiation	Mo*K*α
c (Å)	10.2918(9)	No. of reflections	1564
β(°)	100.186(9)	No. of unique reflections	788
V (Å^3)	507.8(1)	No. $\lvert F_o\rvert > 4\sigma F_o$	663
Space group	*C*2/*m*	R_{az} (%)	2.3 → 1.2
Z	2	R_1 ($\lvert F_o\rvert > 4\sigma F_o$) (%)	4.1
		wR_2 (F_o^2) (%)	5.2

Notes: $R_1 = \Sigma(\lvert F_o\rvert - \lvert F_c\rvert)/\Sigma\lvert F_o\rvert$; $wR_2 = [\Sigma w(F_o^2 - F_c^2)^2/\Sigma w(F_o^2)^2]^{1/2}$, $w = 1/\sigma F_o^2$.

Intensities were corrected for background, absorption, Lorentz, and polarization effects, and reduced to structure factors. Details concerning these procedures are given in Table 2.

The crystal structure was refined using the SHELXTL-PC system of programs; *R* indices are of the form given in Table 2. The structure was refined in the space group *C*2/*m* to an *R*-index of 4.1% for 663 observed reflections. Final atom parameters are given in Table 3, selected interatomic distances and angles are given in Table 4, and refined site-scattering values (epfu) and assigned site-populations (apfu) are given in Table 5. Calculated stereochemical parameters for shirozulite are given in Table 6, and observed and calculated structure factors are listed in Table 7[1].

X-ray powder pattern

Powder diffraction data were collected with a Rigaku Rint-2100V diffractometer using curved-graphite monochromatized Cu*K*α X-rays and operating at 40 kV and 40 mA with a step-width of 0.01 °2θ and a step-interval of 16 s. A Rietveld analysis was done using the program Rietan-2000 (Izumi and Ikeda 2000): the single-crystal structural data described above were used as the initial parameters, and the isotropic-displacement factors were used. Table 8 shows the observed and calculated *d*-values, and the observed intensities; Figure 2 shows the fitted powder-diffraction pattern. Within the estimated standard deviations, the resultant unit-cell parameters are consistent with the values from the single-crystal data.

[1]For a copy of Table 7, document item AM-04-052, contact the Business Office of the Mineralogical Society of America (see inside front cover of recent issue) for price information. Deposit items may also be available on the American Mineralogist web site at http://www.minsocam.org.

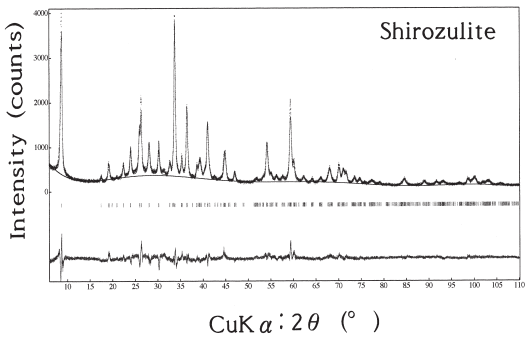

FIGURE 2. Observed (crosses), calculated, and difference powder XRD patterns for shirozulite.

CRYSTAL STRUCTURE

The *T* site

The unit formula calculated from the chemical analysis (Table 1) has 1.464 ^{IV}Al apfu, and the <T-O> distance is 1.668 Å. Figure 3 shows the variation in <T-O> as a function of ^{IV}Al content in some recent structure-refinements of mica. Although some scattering occurs around 1.2 ^{IV}Al, there is a well-developed linear relation between ^{IV}Al content and the <T-O> bond-length. Hazen and Burnham (1973) gave the line: <T-O> = 0.0408 ^{IV}Al + 1.608 [therein $x_{Al}/(x_{Al} + x_{Si})$ is converted to ^{IV}Al]. Both regression lines coincide well, although the line in this study gives slightly shorter values than that given by Hazen and Burnham (1973): 0.001~0.003 Å shorter when ^{IV}Al = 1.0~1.5, respectively, and they coincide at ^{IV}Al = 0.744. The data for shirozulite lie on this trend, indicating that the structure refinement and electron-microprobe results are compatible.

The *M* sites

The relations between mean bond length at the octahedral sites, <M1-O> and <M2-O>, are shown in Figure 4. In almost all samples, the M1 octahedra are larger than the M2 octahedra, and the <M1-O> for almost all trioctahedral micas are less than 2.125 Å (Fig. 4), suggesting that this value is the maximum possible value in these micas.

Dimensional misfit between tetrahedral and octahedral sheets

The structure of shirozulite would seem, at first sight, to be rather unusual relative to other trioctahedral 1M micas, as it has a very large principal octahedrally coordinated cation (Mn^{2+}, r = 0.83 Å; Shannon 1976) *and* a large tetrahedral rotation angle α (8.36°). Donnay et al. (1964) showed that the principal mechanisms whereby the octahedral and tetrahedral layers in mica accommodate their dimensional differences are

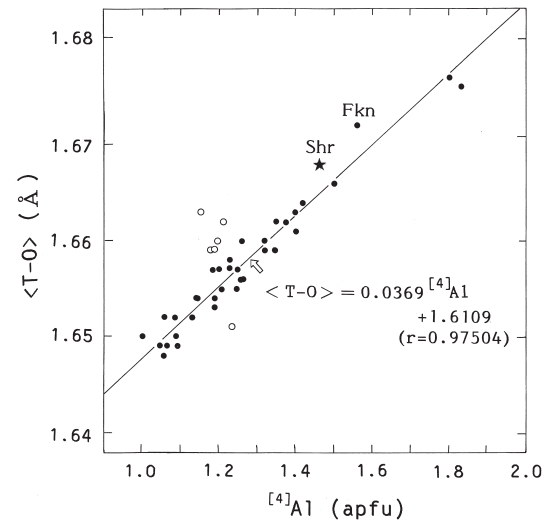

FIGURE 3. <T-O> as a function of ^{IV}Al. Shr(star) = shirozulite (the present study); Fkn = ferrokinoshitalite (Guggenheim and Frimmel 1999). Other data from Hazen and Burnham (1973), Brigatti and Davoli (1990), Brigatti et al. (1991), Brigatti and Poppi (1993), Bigi and Brigatti (1994), Alietti et al. (1995), Brigatti et al. (1998), Hawthorne et al. (1999), Russell and Guggenheim (1999), and Brigatti et al. (2001). Six outliers are shown as unshaded circles. Solid line = a linear least-squares fit to the data, omitting the outliers (r = 0.97504).

octahedral flattening (ψ) and tetrahedral rotation (α). Hazen and Wones (1972) showed that there is an inverse relation between the tetrahedral rotation angle and the mean ionic radius (<*r*>) of the octahedrally coordinated cation(s). In particular, the ideal relation between α and <*r*> (Hazen and Wones 1972) indicates that <*r*> cannot exceed 0.76 Å (i.e. at 0.76 Å, α = 0°), and at larger values of ionic radius, the octahedral sheet should be too large to link to the tetrahedral layer. The mean constituent radius of the octahedrally coordinated cations in shirozulite is 0.76 Å, exactly equal to the maximum size of octahedral cation possible according to the α-<*r*> relation of Hazen and Wones (1972). However, instead of α being equal to 0°, as predicted for this specific ionic radius, α = 8.36°, one of the largest values of α observed in trioctahedral micas (Table 6, Fig. 5). How can the octahedral layer in shirozulite link to the tetrahedral layer with such a large value of tetrahedral rotation? First, the octahedral flattening in shirozulite is small compared with most other trioctahedral micas (Fig. 6), effectively reducing the size of the octahedral layer. Second, the tetrahedral layer in shirozulite contains significantly more Al (1.46) than the 1.00 Al *apfu* present in the synthetic trioctahedral micas considered by Hazen and Wones (1972). This additional ^{IV}Al increases the size of the tetrahedral

TABLE 3. Final parameters for the crystal structure of shirozulite

Atom	x	y	z	U_{eq}*	U_{11}	U_{22}	U_{33}	U_{23}	U_{13}	U_{12}
Si	0.5754(2)	0.16685(4)	0.22491(14)	126(4)	108(6)	63(6)	207(7)	–3(5)	28(5)	0(5)
Mn1	0	0.5	0.5	113(6)	82(9)	38(8)	222(11)	0	34(7)	0
Mn2	0	0.83113(15)	0.5	117(4)	79(6)	49(6)	222(8)	0	27(5)	0
K	0	0	0	319(8)	335(13)	273(12)	344(14)	0	48(10)	0
O1	0.8265(7)	0.2288(4)	0.1681(4)	218(12)	178(18)	186(19)	30(2)	–31(17)	62(15)	–65(15)
O2	0.5141(11)	0	0.1678(6)	213(17)	25(3)	9(2)	28(3)	0	-8(23)	0
O3	0.6303(7)	0.1675(4)	0.3885(4)	163(10)	161(16)	105(15)	219(18)	6(14)	19(14)	4(14)
O4	0.1283(11)	0	0.3949(6)	191(16)	18(3)	19(3)	20(3)	0	20(20)	0
H	0.105(18)	0	0.2982(8)	100(–)						

* $\times 10^4$.

TABLE 4. Interatomic distances (Å) and angles (°) in shirozulite

T-O1	1.667(4)	M1-O3a	×4	2.128(4)	M2-O3a	×2	2.102(4)
T-O1a	1.674(4)	M1-O4a	×2	2.099(5)	M2-O3b	×2	2.113(3)
T-O2	1.674(3)	<M1-O>		2.118	M2-O4c	×2	2.095(4)
T-O3	1.657(4)				<M2-O>		2.103
<T-O>	1.668						
		M1 shared			M2 shared		
O1-O1a	2.718(6)	O3-O3	×2	2.893(8)	O3-O3		2.893(8)
O1-O2	2.715(6)	O3-O4	×4	2.841(6)	O4-O4		2.764(13)
O1-O3	2.726(6)	(mean)		2.858	O3-O3	×2	2.871(7)
O1a-O2	2.722(5)	M1 unshared			O3-O4	×2	2.841(6)
O1a-O3	2.728(5)	O3-O3	×2	3.122(8)	(mean)		2.847
O2-O3	2.736(6)	O3-O4	×4	3.130(6)	M2 unshared		
mean	2.724	(mean)		3.127	O3-O3	×2	3.098(4)
		mean		2.993	O3-O4	×2	3.091(6)
O1-T-O1a	108.9(2)				O3-O4	×2	3.099(4)
O1-T-O2	108.7(2)	M1 shared			(mean)		3.096
O1-T-O3	110.2(2)	O3-M1-O3	×2	85.6(2)	mean		2.971
O1a-T-O2	108.7(2)	O3- M1-O4	×4	84.4(1)			
O1a-T-O3	109.9(2)	(mean)		84.8	M2 shared		
O2-T-O3	110.4(2)	M1 unshared			O3-M2-O3		87.0(2)
mean	109.5	O3-M1-O3	×2	94.4(2)	O4-M2-O4		82.6(3)
		O3-M1-O4	×4	95.6(1)	O3-M2-O3	×2	85.9(1)
K-O1e	×4 2.997(4)	(mean)		95.2	O3-M2-O4	×2	84.9(2)
K-O2	×2 2.990(6)	mean		90.0	(mean)		85.2
<K-O>inner	2.995				M2 unshared		
K-O1d	×4 3.375(4)				O3-M2-O3	×2	94.6(1)
K-O2f	×2 3.378(7)				O3-M2-O4	×2	94.5(1)
<K-O>outer	3.376				O3-M2-O4	×2	95.2(2)
mean	3.185	O4-H		0.98(10)	(mean)		94.8
					mean		90.0
O1-O1a-O1	163.3(3)						

Notes: a = 1/2 + x – 1, 1/2 + y, z; b = 1 – x, 1 – y, 1 – z; c = x, 1 + y, z; d = x – 1, y, z; e = 1/2 + x – 1, 1/2 + y – 1, z; f = –x, y, –z.

TABLE 5. Refined site-scattering (epfu) and assigned site-populations (apfu)

Site	Refined site -scattering value		Assigned site-populations		Calculated site -scattering value
Si	56		2.54 Si + 1.46 Al		54.5
M1	19.8(2)	} 57.7	0.04 Ti + 0.29 Al + 0.20 Fe^{2+}	} 59.3	
M2	37.9(3)		+ 0.94 Mg + 1.53 Mn		
K	23.1(3)		0.90 K + 0.09 Ba		22.1

TABLE 6. Calculated structure parameters for shirozulite

Parameter	Value
α (°)*	8.36
ψ (°)† M1	58.5
M2	58.2
T_{tet} (°)‡	110.2
Sheet thickness §	
octahedral (Å); t_o	2.216
tetrahedral (Å); t_t	2.224
Interlayer separation (Å); t_i	3.468
Δ (Å) ‖	0.479
<K-O> (outer) – <K-O> (inner) (Å)	0.381
β_{ideal} (°)#	100.02

* $\tan\alpha = 4b(0.25 - y_{01})/a$ (Hazen and Burnham 1973).
† $\cos\psi = t_o/(2d_0)$, $t_o = 2\{0.5 - [2z_{03} + z_{04}]/3\}c\sin\beta$, d_o = <M-O> (Hazen and Burnham 1973).
‡ mean O_{basal} – T-O_{apical}.
§ $t_o = 2d_o\cos\psi$, $t_t = 4d_t/3$, $t_i = c\sin\beta - 2d_o\cos\psi - (8/3)d_t$ (Donnay et al. 1964).
‖ Dimensional misfit between tetrahedral and octahedral sheets defined as $\Delta = \{2\sqrt{3}<O_{bas} - O_{bas}> - 3\sqrt{2}d_o\}$ (Toraya 1981).
180° – $\cos^{-1}[a/(3c)]$ (Tyrna and Guggenheim 1991).

layer, promoting linkage between the tetrahedral layer and a large octahedral layer. Increasing amounts of octahedrally coordinated Al will have a similar effect. These arguments account for the large tetrahedral rotation in shirozulite, and also suggest that end-member shirozulite, K Mn_3^{2+} Al Si_3 O_{10} $(OH)_2$, will not be stable as the octahedral layer is very large without any compensating increase in the size of the tetrahedral layer.

TABLE 8. Indexed powder pattern for shirozulite

h k l	d_{obs}	d_{calc}	I_{obs}
0 0 1	10.09	10.16	100
0 0 2	5.05	5.079	9
0 2 0	4.638	4.666	15
1 1 0	4.590	4.6123	14
$\bar{1}$ 1 1	4.447	4.4693	8
0 2 1	4.235	4.2400	9
1 1 1	3.962	3.9735	14
$\bar{1}$ 1 2	3.699	3.7139	22
0 2 2	3.426	3.4361	33
0 0 3	3.376	3.3860	51
1 1 2	3.170	3.1775	27
$\bar{1}$ 1 3	2.946	2.9576	22
0 2 3	2.736	2.7404	16
$\bar{1}$ 3 1	2.646	2.6544	96
0 0 4	2.536	2.5395	18
$\bar{1}$ 3 2	2.458	2.4666	46
$\bar{2}$ 2 1	2.323	2.3284	14
2 2 0	2.296	2.3061	16
$\bar{2}$ 0 3	2.287	2.2972	18
1 3 2	2.278	2.2887	16
$\bar{1}$ 3 3	2.194	2.2023	36
0 4 2	2.121	2.1200	9
0 0 5	2.028	2.0316	20
1 3 3	2.0201	2.0162	21
$\bar{1}$ 3 4	1.9279	1.9339	11
1 5 0	1.7609	1.7606	8
1 5 1	1.7161	1.7177	8
$\bar{3}$ 1 3	1.6673	1.6697	10
1 5 2	1.6327	1.6338	9
2 4 2	1.5956	1.5989	8
$\bar{3}$ 3 1	1.5537	1.5563	48
3 3 0	1.5350	1.5374	18
$\bar{1}$ 3 6	1.4865	1.4941	8
0 0 7	1.4491	1.4511	7
$\bar{3}$ 3 4	1.4152	1.4163	7
3 3 2	1.4115	1.4119	7
$\bar{2}$ 0 7	1.3786	1.3814	11
1 3 6	1.3755	1.3768	12

Notes: Results of Rietveld refinement using RIETAN-2000 (Izumi and Ikeda 2000): intensity data were collected by Rigaku Rint-2100V ; graphite monochromated Cu*K*α X-ray radiation at 40 kV–40 mA; slit system 1/2°–0.15 mm–1/2°; 25 × 15 × 1 mm glass holder; step width = 0.01°(2θ), collecting times = 16s per step; 2θ range = 6–110°. Rwp = 9.55%, RP = 7.65%, Re = 5.26%, S = 1.8149. a = 5.3925(7), b = 9.332(1), c = 10.324(1) Å, β = 100.301(7)°, *V* = 511.2(1)Å^3.

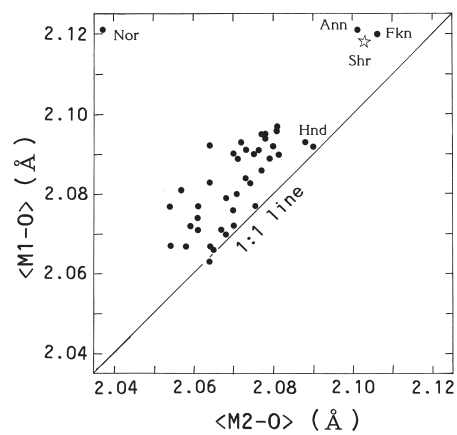

FIGURE 4. <M1-O> and <M2-O> relations. Nor = norrishite (Tyrna and Guggenheim 1991); Hnd = hendricksite (Robert and Gasperin 1985); Fkn = ferrokinoshitalite (Guggenheim and Frimmel 1999); Ann = annite (Hazen and Burnham 1973); Shr(star) = shirozulite (the present study). Other data from Brigatti and Davoli (1990), Brigatti et al. (1991), Brigatti and Poppi (1993), Bigi and Brigatti (1994), Alietti et al. (1995), Brigatti et al. (1998), Hawthorne et al. (1999), Russell and Guggenheim (1999), Schingaro et al. (2001), and Brigatti et al. (2001).

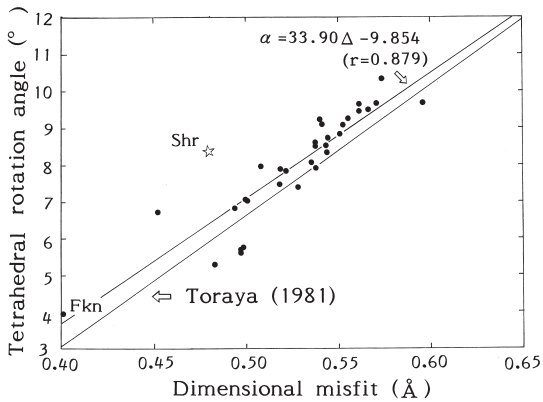

FIGURE 5. Tetrahedral rotation angle as a function of dimensional misfit between tetrahedral and octahedral sheets. Fkn = ferrokinoshitalite (Guggenheim and Frimmel 1999); Shr (star) = shirozulite (the present study); Regression line = Toraya (1981). Other data from Cruciani and Zanazzi (1994), Brigatti et al. (1998), and Schingaro et al. (2001).

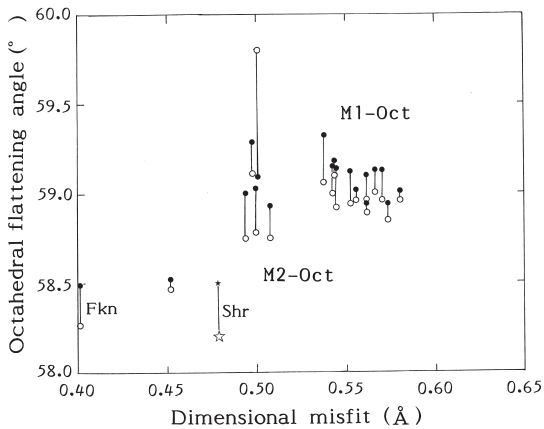

FIGURE 6. Octahedral flattening angle as a function of dimensional misfit between tetrahedral and octahedral sheets. Fkn = ferrokinoshitalite (Guggenheim and Frimmel 1999); Shr (star) = shirozulite (the present study); other data from Cruciani and Zannazzi (1994), Brigatti et al. (1998), and Schingaro et al. (2001).

The interlayer site

The interlayer site in shirozulite contains significant K and Ba, and the refined site-scattering value of 23.1 epfu is in excellent accord with the effective scattering value of 22.1 epfu calculated from the unit formula (Table 5). The interlayer-cation site occurs between the T-O-T (tetrahedral-octahedral-tetrahedral) layers that stack in the **z** direction. Thus, both variation in size and charge of the constituent interlayer cations will strongly affect the interlayer separation and the *c*-dimension of the unit cell. In *C*2/*m* 1*M* annite, the interlayer separations (3.35–3.37 Å; α = 1.5–2.0°) are somewhat smaller than in analogous Mg-rich micas (3.45–3.48 Å; α = 8.9–10.2°) (Bailey 1984; Brigatti and Guggenheim 2002); the interlayer separation and tetrahedral rotation in shirozulite, are similar to those in Mg-rich micas. There is an inverse relation between tetrahedral rotation and interlayer separation (see Fig. 15 in Brigatti and Guggenheim 2002), but there are significant perturbations from a monotonic relation; these are presumably due to factors that affect the relative dimensions of the tetrahedral and octahedral layers, e.g., F content, variation in T-site populations (Al, Fe^{3+} substituting for Si), variation in tri- and tetra-valent cation content of the octahedral sites, and type of interlayer cation. Further studies are needed to untangle the effects of these variations on linkage of the tetrahedral and octahedral layers.

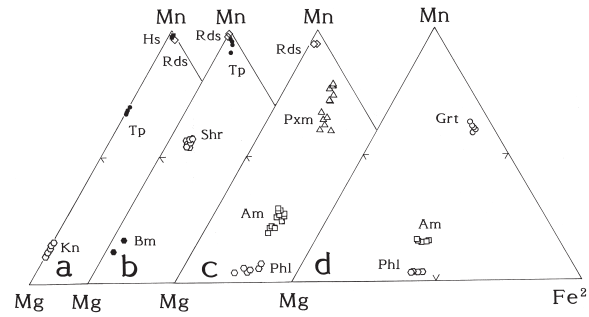

FIGURE 7. Chemical compositions of minerals in the Mg-Fe^{2+}-Mn^{2+} system. (**a**) hausmannite-tephroite ore. (**b**) tephroite-rhodochrosite ore. (**c**) pyroxmangite-manganocummingtonite ore. (**d**) garnet-manganocummingtonite ore. Kn = kinoshitalite; Tp = tephroite; Hs = hausmannite; Rds = rhodochrosite; Bm = bementite; Shr = shirozulite; Phl = phlogopite; Am =amphibole; Pxm = pyroxmangite; Grt = garnet.

ELEMENT PARTITION AMONG COEXISTING MINERALS

Chemical compositions of trioctahedral micas of the manganno-barian phlogopite-kinoshitalite series are strongly dependent on the different types of coexisting minerals (Fig. 7), particularly with regard to the $^{XII}Ba^{IV}Al^{XII}K_{-1}{}^{IV}Si_{-1}$ substitutions in the kinoshitalite-annite series. Kinoshitalite occurs in hausmannite-rhodochrosite ores in which Mn is the predominant transition-metal cation, but its octahedral sites are rich in Mg rather than Mn, and contain negligible Fe^{2+} and Fe^{3+} (Fig. 7a). Shirozulite occurs in rhodochrosite-tephroite ore (Fig. 7b). However, micas in rhodochrosite-tephroite ore are generally of mangano-barian phlogopite compositions, and its octahedral Mn are usually under one-third. Micas that coexist with pyroxmangite, manganoan cummingtonite-grunerite amphiboles, and/or garnet are commonly rich in Fe^{2+}, and they belong to the manganoan phlogopite-annite series (Figs. 7c and 7d). Judging from the chemical compositions of the coexisting minerals, it is supposed that the minerals are in chemical equilibrium (at least the manganese or manganoan-silicate minerals). As the chemical compositions of garnets are in the spessartine-almandine-grossular system (Mn-Fe^{2+}-Ca) and have a low pyrope component (Mg), mineral formation is assumed to have occurred at low pressure.

To compare the element distributions of the trioctahedral mica with coexisting silicate minerals (i.e., monoclinic amphibole, pyroxmangite, olivine, and garnet), we examined the apparent partition coefficients of these minerals. We may define the apparent partition coefficients between, for example, garnet, and trioctahedral mica for Mg-Mn and Fe^{2+}-Mn as follows:

$$K'_{DMg\text{-}Mn} = (X_{Mg}/X_{Mn})^{Phl} / (X_{Mg}/X_{Mn})^{Grt}$$
$$K'_{DFe\text{-}Mn} = (X_{Fe}/X_{Mn})^{Phl} / (X_{Fe}/X_{Mn})^{Grt}$$
$$\text{and } K'_{DMg\text{-}Fe} = (X_{Mg}/X_{Fe})^{Phl} / (X_{Mg}/X_{Fe})^{Grt} = K'_{DMg\text{-}Mn} / K'_{DFe\text{-}Mn}$$

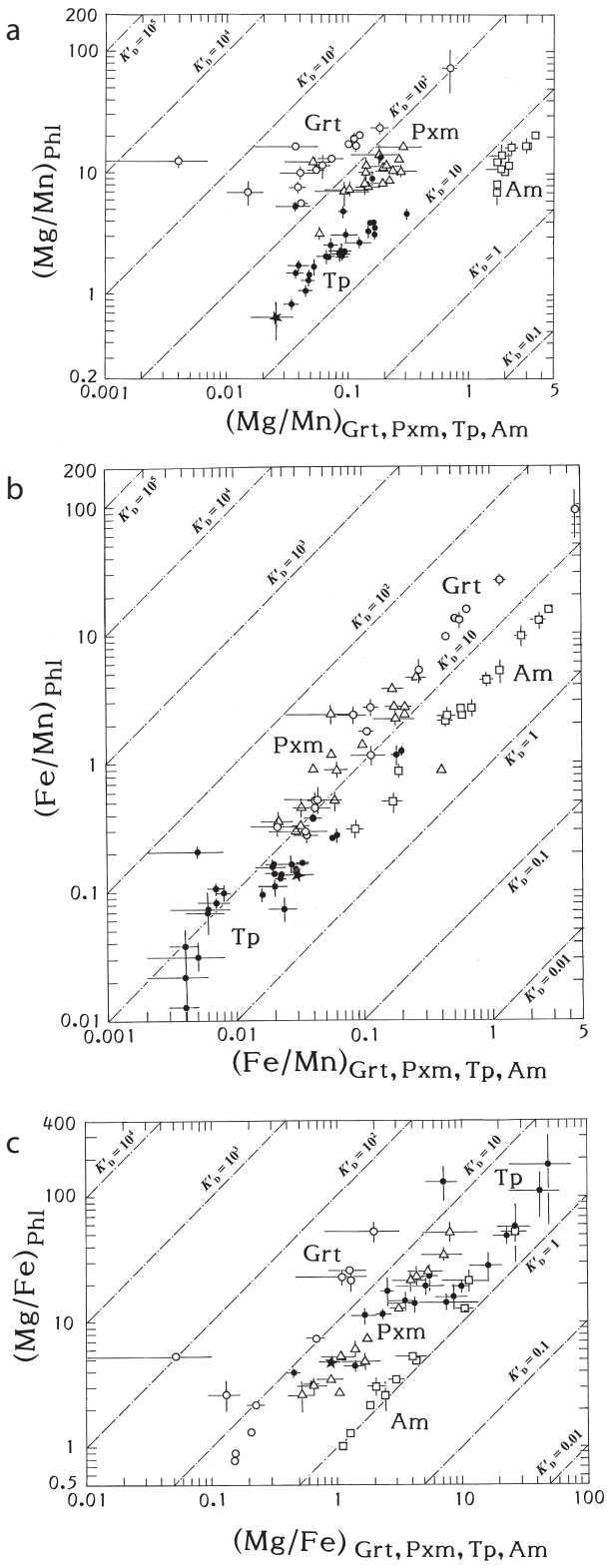

FIGURE 8. Partition of cations among coexisting minerals. amphiboles = Am, open squares. tephroite = Tp, solid circles. pyroxmangite = Pxm, triangles. garnet = Grt, open circles. (**a**) Mg/Mn^{2+}. (**b**) Fe^{2+}/Mn^{2+}. (**c**) Mg/Fe^{2+}. Solid star = shirozulite-tephroite.

where X_{Mg}, X_{Mn}, and X_{Fe} denote the mole fraction of Mg, Mn, and Fe^{2+} end-members of the relevant solid solutions, and superscripts Phl = mica and Grt = garnet. These K values correspond to the exchange reactions of the following type:

$$R_3Al_2Si_3O_{12} + KMn_3AlSi_3O_{10}(OH)_2 = Mn_3Al_2Si_3O_{12} + KR_3AlSi_3O_{10}(OH)_2$$

where R denotes Mg or Fe^{2+}. Supposing that mineral-formation conditions (i.e., temperature, pressure, and H_2O fugacity) were the same, but the chemical potentials were different in each zone, and supposing also that each coexisting mineral can be treated as an ideal solid solution, the same K_D^n values would apply for each set of element- and mineral-pairs.

Element distribution among coexisting minerals is shown in Figures 8a, 8b, and 8c. Samples are from Japanese thermally metamorphosed strata-bounded Mn ore deposits with formation conditions (*T-P*) similar to those of the Taguchi mine: Noda-Tamagawa mine, Iwate Pref.; Tatehira mine, Hokkaido; Kuranosawa mine, Tochigi Pref.; Hamayokogawa mine, Gunma Pref.; Hokkejino mine, Kyoto; Fukumigawa mine, Ehime Pref.; and Shimozuru mine, Miyazaki Pref. Relative to Mn^{2+}, Mg preferentially partitions into coexisting minerals in the following order: micas (octahedral sites, M1 and M2) > manganoan cummingtonite-grunerite (M1, M2, M3, and M4 sites) > tephroite (M1 and M2 sites) > pyroxmangite (M sites) > garnet (dodecahedral site) (Fig. 8a). Iron (Fe^{2+}) more easily replaces Mn^{2+} than Mg, and shows the following preference: micas > amphiboles > tephroite > pyroxmangite > garnet (Fig. 8b). Substitution of Mg and Fe^{2+} in coexisting minerals is more extensive, and Mg shows the preference: micas > amphiboles > tephroite > pyroxmangite > garnet (Fig. 8c). Mn^{2+} normally partitions preferentially into other minerals relative to mica, and hence shirozulite will seldom occur in ordinary parageneses.

ACKNOWLEDGMENTS

The authors thank Y. Motomura and M. Shimada (Kyushu University) for help with the Vickers hardness measurement, M. Cooper (University of Manitoba) for collection of the X-ray data, and Y. Aoki, I. Shinno, Y. Nakamuta, S. Uehara, and Y. Kuwahara (Kyushu University) for their critical reviews of this manuscript. Constructive comments by M. Fleet, G. Harlow, and B.E. Owens are greatly acknowledged. FCH was supported by a Canada Research Chair in Crystallogpaphy and Mineralogy and by Major Installation, Major Equipment and Discovery grants from the Natural Sciences and Engineering Research Council of Canada.

REFERENCES CITED

Alietti, E., Brigatti, M.F., and Poppi, L. (1995) The crystal structure and chemistry of high-aluminium phlogopite. Mineralogical Magazine, 59, 149–157.

Bailey, S.W. (1984) Crystal chemistry of the true micas. In S.W. Bailey, Ed., Micas, 13, 13–60. Reviews in Mineralogy, Mineralogical Society of America, Washington, D.C.

Bigi, S. and Brigatti, M.F. (1994) Crystal chemistry and microstructures of plutonic biotite. American Mineralogist, 79, 63–72.

Brigatti, M.F. and Davoli, P. (1990) Crystal-structure refinements of *1M* plutonic biotites. American Mineralogist, 75, 305–313.

Brigatti, M.F. and Guggenheim, S. (2002) Mica crystal chemistry and the influence of pressure, temperature, and solid solution on atomistic models. In A. Mottana, F. P. Sassi, J. B. Thompson Jr., and S. Guggenheim, Eds., Micas: crystal chemistry and metamorphic petrology, 46, 1–97. Reviews in Mineralogy and Geochemistry, Mineralogical Society of America, Washington, D.C.

Brigatti, M.F. and Poppi, L. (1993) Crystal chemistry of Ba-rich trioctahedral micas-1*M*. European Journal of Mineralogy, 5, 857–871.

Brigatti, M.F., Galli, E., and Poppi, L. (1991) Effect of Ti substitution in biotite-*1M* crystal chemistry. American Mineralogist, 76, 1174–1183.

Brigatti, M.F., Lugli, C., Poppi, L., and Elburg, M. (1998) Crystal chemistry of biotites from mafic enclaves in the Warburton granodiorite, Lachlan Fold Belt (Australia). European Journal of Mineralogy, 10, 855–864.

Brigatti, M.F., Medici, L., Poppi, L., and Vaccaro, C. (2001) Crystal chemistry of trioctahedral micas-*1M* from the Alto Paranaiba igneous province, Southeastern Brazil. Canadian Mineralogist, 39, 1333–1345.

Cruciani, G. and Zanazzi, P.F. (1994) Cation partitioning and substitution mechanisms in 1*M* phlogopite: A crystal chemical study. American Mineralogist, 79, 289–301.

Donnay, G., Donnay, J.D.H., and Takeda, H. (1964) Trioctahedral one-layer micas. Prediction of the structure from composition and cell dimensions. Acta Crystallographica, 17, 1374–1381.

Guggenheim, S. and Frimmel, H.E. (1999) Ferrokinshitalite, A new species of brittle mica from the Broken Hill mine, South Africa: Structural and mineralogical characterization. Canadian Mineralogist, 37, 1445–1452.

Hawthorne, F.C., Teertstra, D.K., and Černý, P. (1999) Crystal-structure refinement of a rubidian cesian phlogopite. American Mineralogist, 84, 778–781.

Hazen, R.M. and Burnham, C.W. (1973) The crystal structures of one-layer phlogopite and annite. American Mineralogist, 58, 889–900.

Hazen, R.M. and Wones, D.R. (1972) The effect of cation substitutions on the physical properties of trioctahedral micas. American Mineralogist, 57, 103–129.

Hirowatari, F. and Isono, K. (1963) Yoshimuraite from the manganese ore deposits of Taguchi mine, Aichi Prefecture. Journal of the Mineralogical Society of Japan, 6, 230–243 (In Japanese).

Izumi, F. and Ikeda, T. (2000) Multi-purpose pattern-fitting system RIETAN-2000 and its applications to micro porous materials. Journal of Crystallographic Society of Japan, 42, 516–521.

Robert, J.-L. and Gasperin, M. (1985) Crystal structure refinement of hendricksite, a Zn- and Mn-rich trioctahedral potassium mica: a contribution to the crystal chemistry of zinc-bearing minerals. Tschermaks Mineralogische und Petrographische Mitteilungen, 34, 1–14.

Russell, R.L. and Guggenheim, S. (1999) Crystal structures of near-end-member phlogopite at high temperatures and heat-treated Fe-rich phlogopite: The influence of the O, OH, F site. Canadian Mineralogist, 37, 711–720.

Schingaro, E., Scordari, F., and Ventruti, G. (2001) Trioctahedral micas-1*M* from Mt. Vulture (Italy): Structural disorder and crystal chemistry. European Journal of Mineralogy, 13, 1057–1069.

Shannon, R.D. (1976) Revised effective ionic radii and systematic studies of interatomic distances in halides and chalcogenides. Acta Crystallographica, A32, 751–767.

Shoda, T. and Bunno, M. (1973) Optical rotation axes in a manganoan richterite from the Taguchi mine, Aichi Prefecture, Japan. Mineralogical Journal, 7, 159–168.

Toraya, H. (1981) Distortions of octahedra and octahedral sheets in 1M micas and the relation to their stability. Zeitschrift für Kristallographie, 157, 173–190.

Tyrna, P.L. and Guggenheim, S. (1991) The crystal structure of norrishite, $KLiMn_2^{3+}Si_4O_{12}$: An oxygen-rich mica. American Mineralogist, 76, 266–271.

Manuscript received June 5, 2002
Manuscript accepted September 19, 2003
Manuscript handled by Brent Owens